

Supplementary materials: (Figures)

1)- Covalent bonds

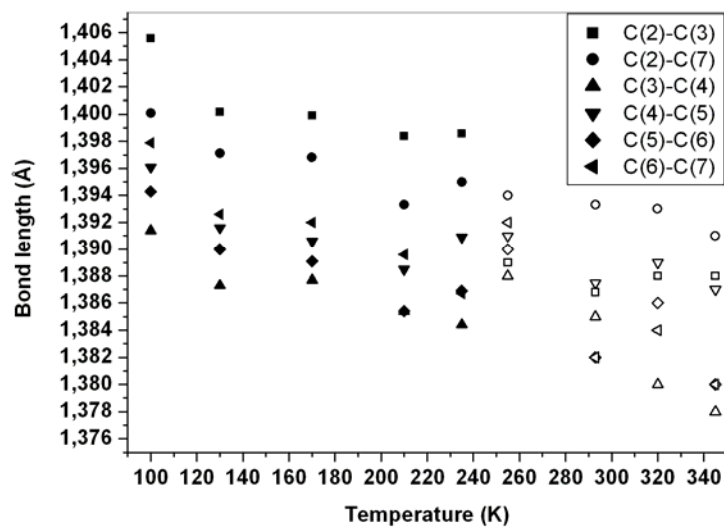


Figure 4-a. The $C_{sp^2} - C_{sp^2}$ bond length variation versus temperature.

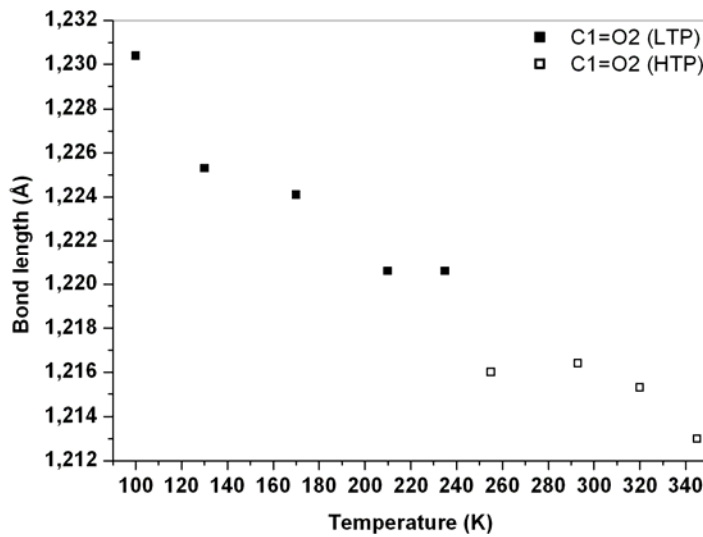


Figure 4-b. The C1=O2 bond length variation versus temperature

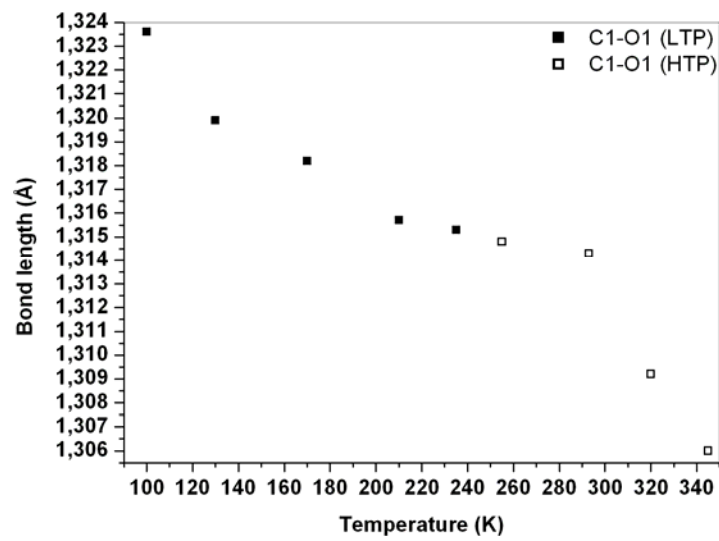


Figure 4-c. The C1—O1 bond length variation versus temperature.

2)- Hydrogen bonds

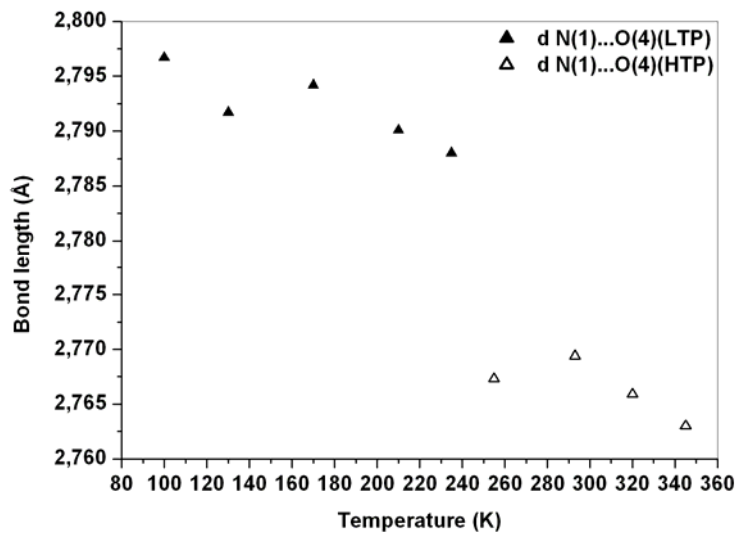


Figure 5-c. The variation of the N1...O4 distance versus temperature.

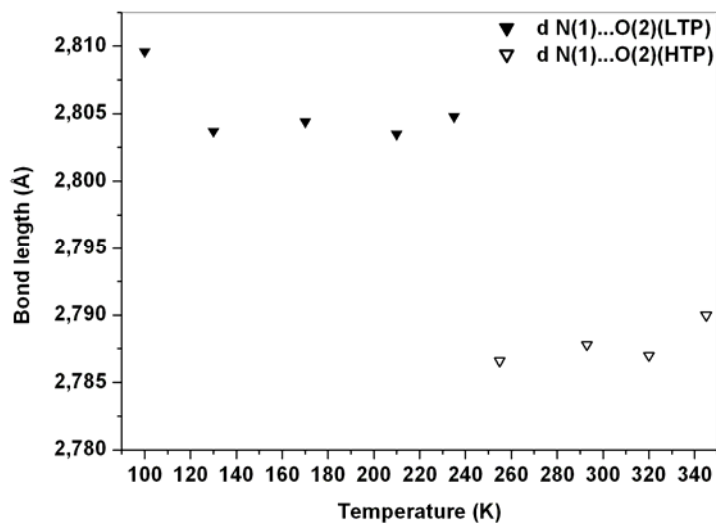


Figure 5-d. The variation of the N1...O2 distance versus temperature.

3)- Isotropic displacement parameters (U_{eq})

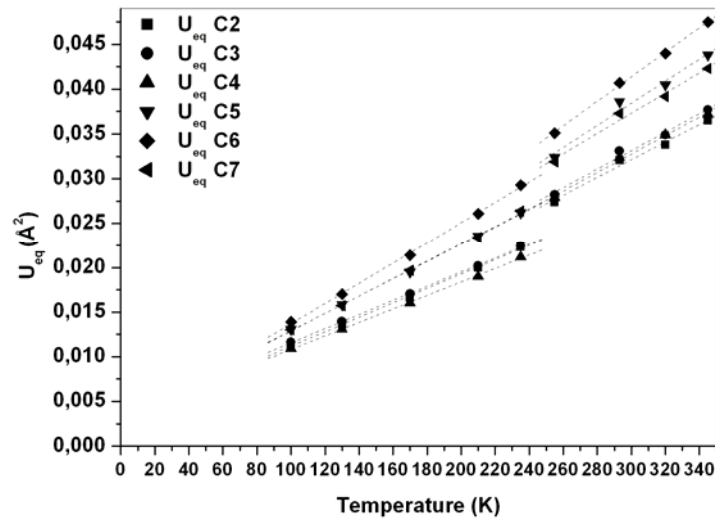


Figure 6-a. Evolution of the isotropic thermal displacement parameters for the organic cation.

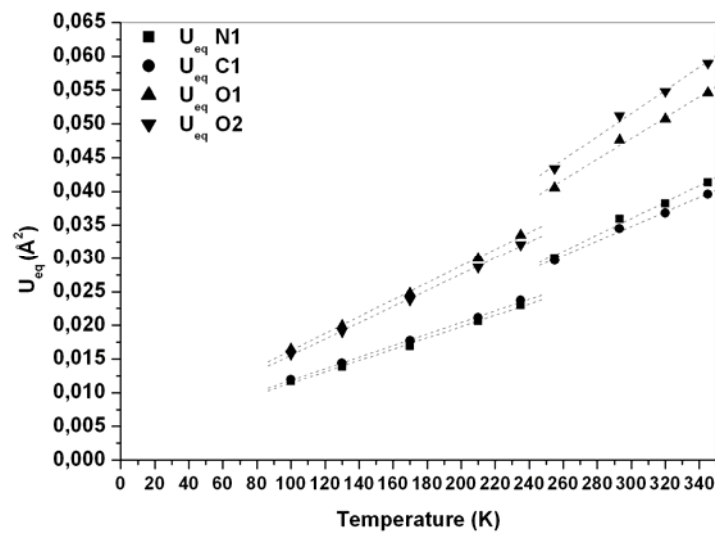


Figure 6-b. Evolution of the isotropic thermal displacement parameters for the organic cation.

3)- Anisotropic displacement parameters (U^{ii})

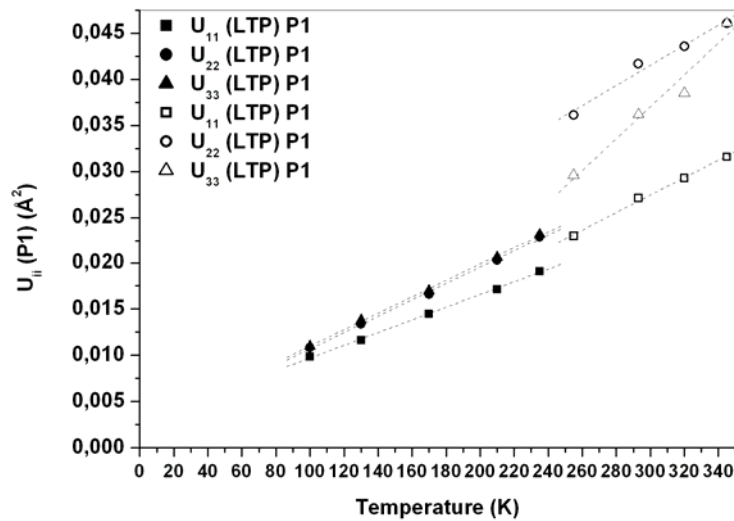


Figure 7-a. The change with temperature of the principal anisotropic displacement parameter U^{ii} for the P1 atom.

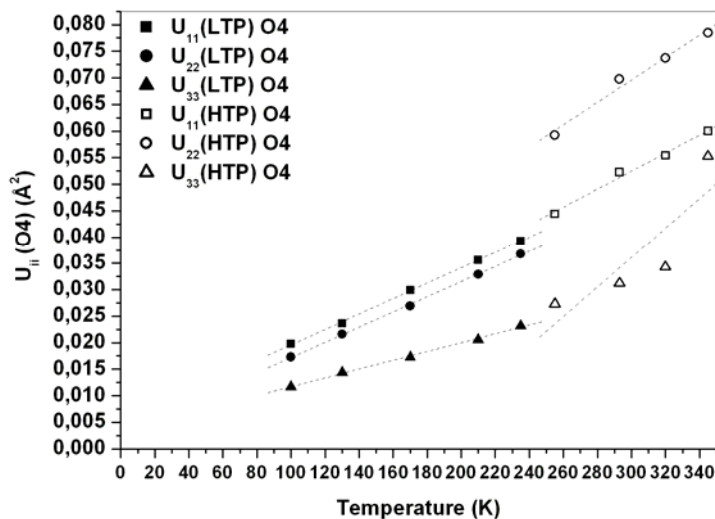


Figure 7-b. The change with temperature of the principal anisotropic displacement parameter U^{ii} for the O4 atom.

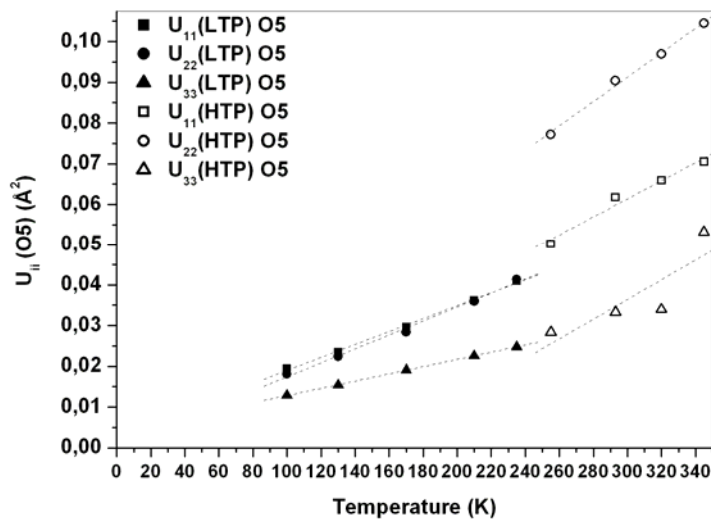


Figure 7-c. The change with temperature of the principal anisotropic displacement parameter U^{ii} for the O5 atom.

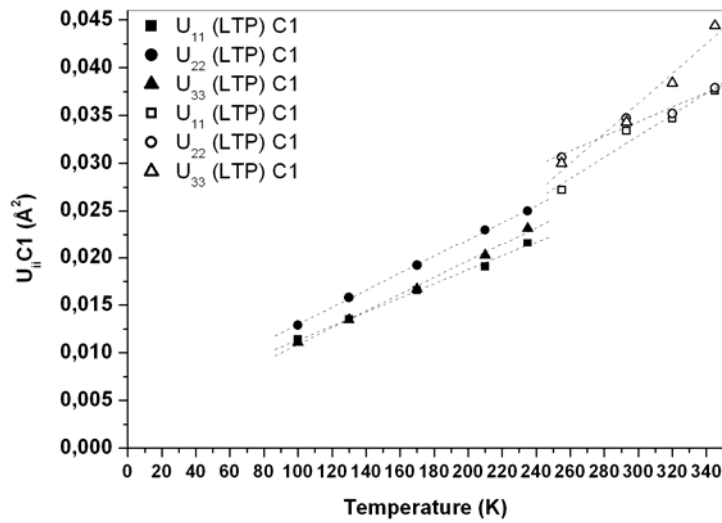


Figure 7-d. The change with temperature of the principal anisotropic displacement parameter U^{ii} for the C1 atom.

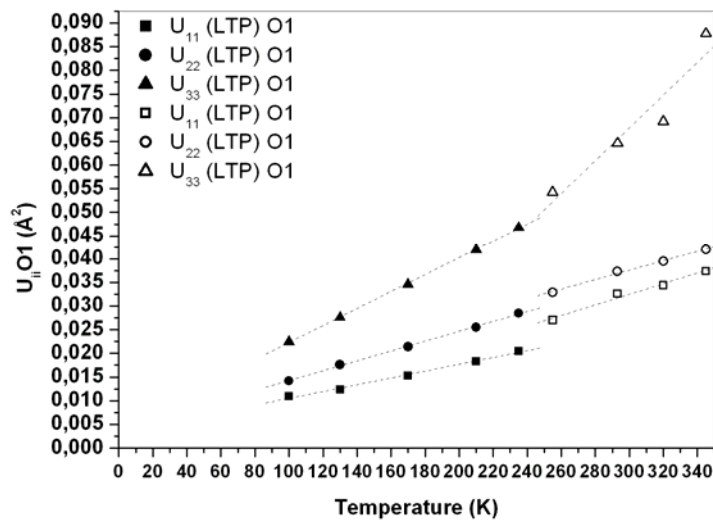


Figure 7-e. The change with temperature of the principal anisotropic displacement parameter U^{ii} for the O1 atom.

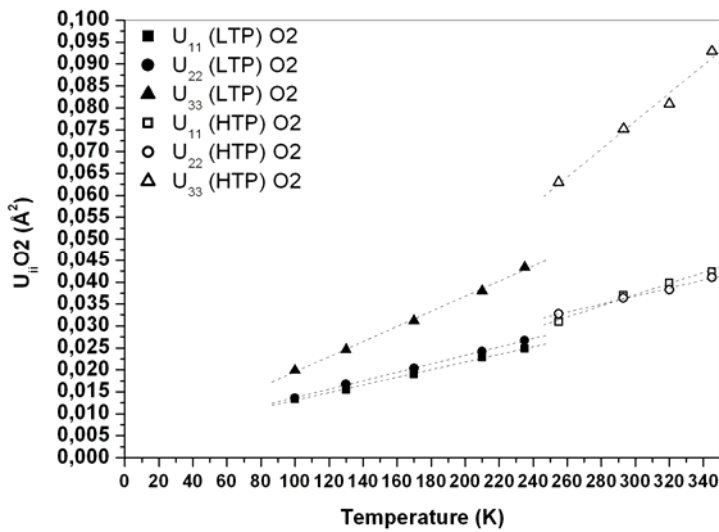


Figure 7-f. The change with temperature of the principal anisotropic displacement parameter U^{ii} for the O2 atom.

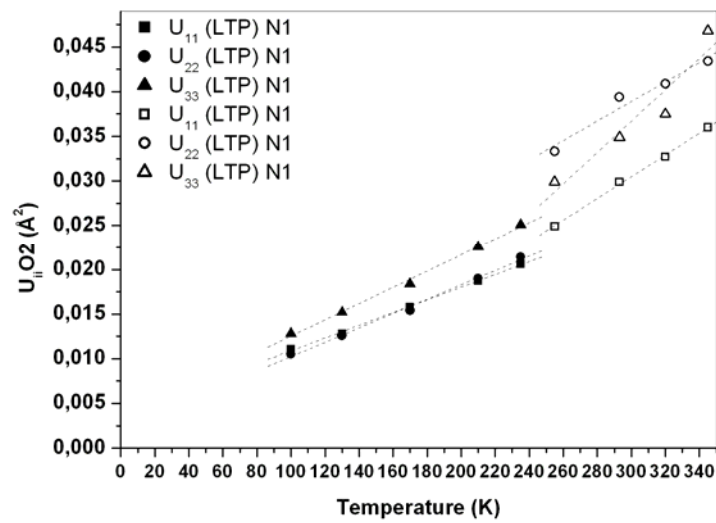


Figure 7-g. The change with temperature of the principal anisotropic displacement parameter U^{ii} for the N1 atom.

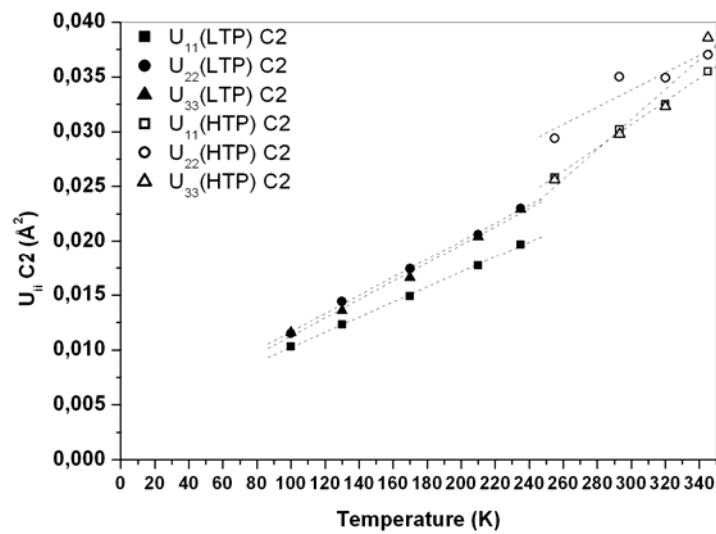


Figure 7-h. The change with temperature of the principal anisotropic displacement parameter U^{ii} for the C2 atom.

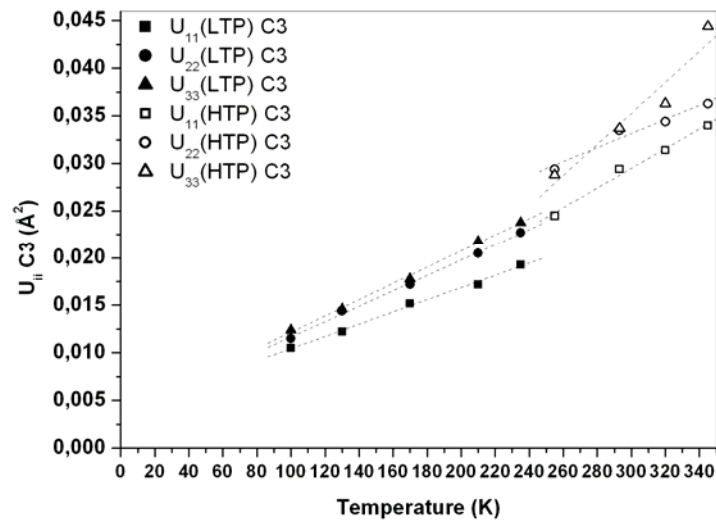


Figure 7-i. The change with temperature of the principal anisotropic displacement parameter U^{ii} for the C3 atom.

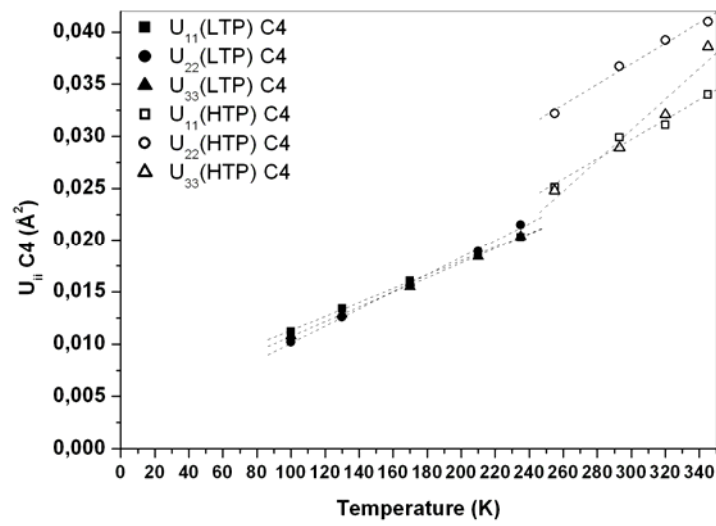


Figure 7-j. The change with temperature of the principal anisotropic displacement parameter U^{ii} for the C4 atom.

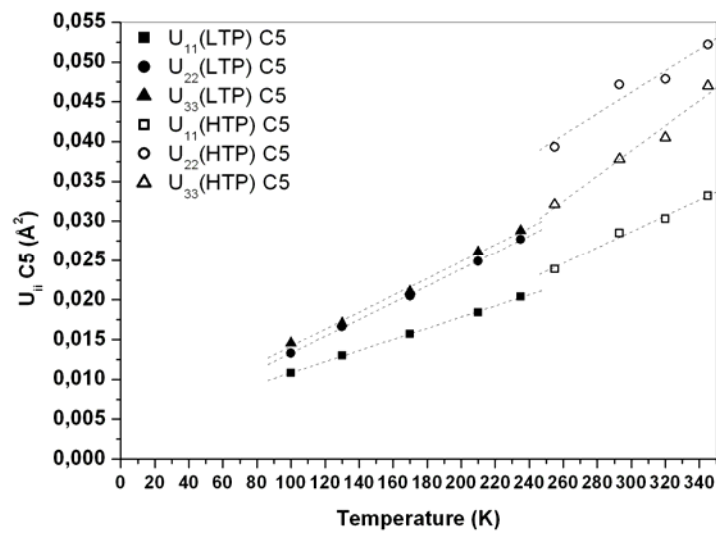


Figure 7-k. The change with temperature of the principal anisotropic displacement parameter U^{ii} for the C5 atom.

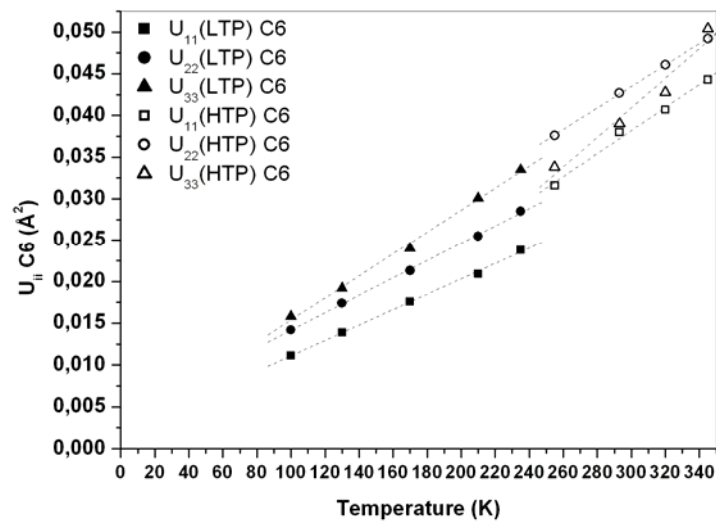


Figure 7-l. The change with temperature of the principal anisotropic displacement parameter U^{ii} for the C6 atom.

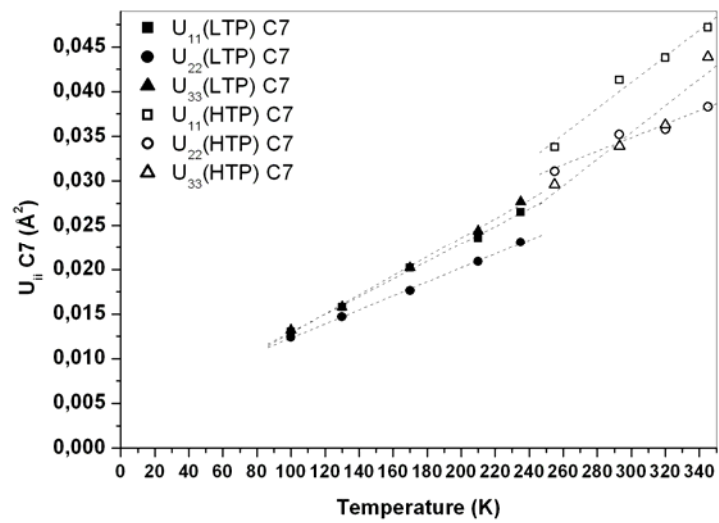


Figure 7-m. The change with temperature of the principal anisotropic displacement parameter U^{ii} for the C7 atom.

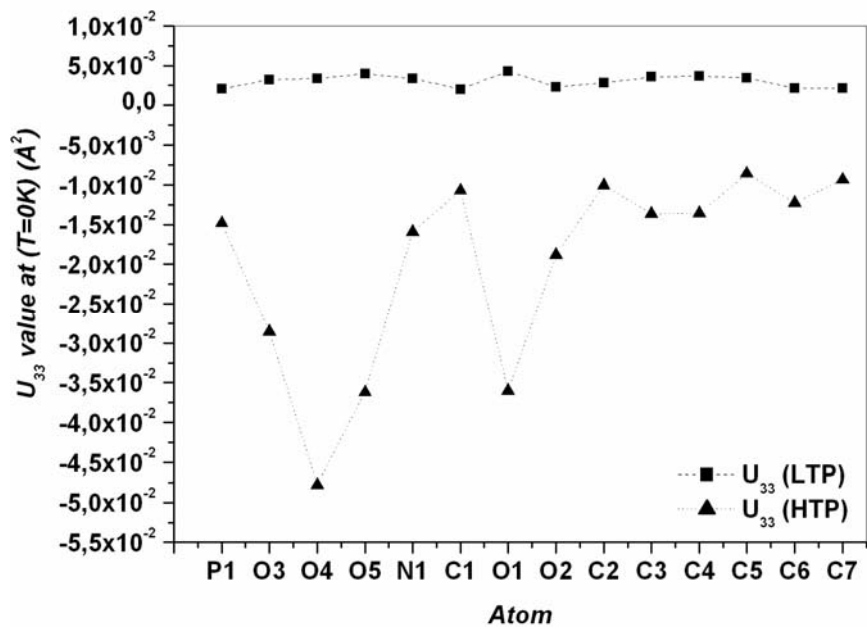


Figure 7-n. Extrapolated values at $T = 0$ K of the U^{33} parameters for all non-H atoms.

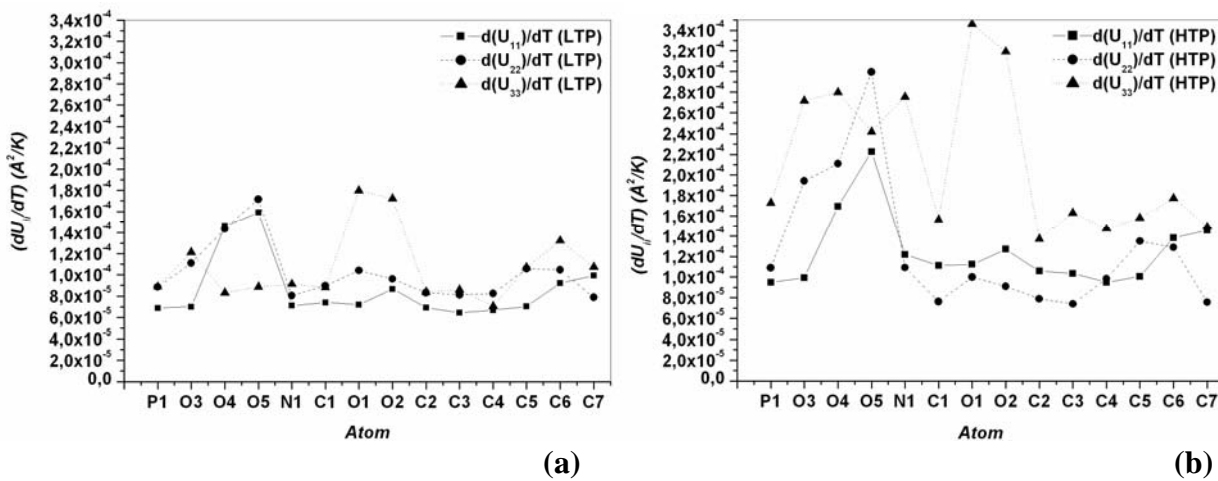


Figure 7-o. Slopes variations for all non-H atoms in (a) (LTP) and (b) (HTP).

The slope (dU^{ii}/dT) for all non-H atoms in both phases (LTP) and (HTP) is calculated from the linear variation of U^{ii} versus temperature. For LTP in the range 100-246K and 246-345K for HTP.

This graph (**Figure 7-o**) reveals some interesting features: the slope does not behave in the same way for all atoms and therefore both ions do not behave as rigid bodies. The most important slope variations, in both phases, concern the U^{22} and U^{33} coefficients of the O5, O1 and O2 oxygen atoms. The U^{22} slopes increase by a third at the (LTP) \rightarrow (HTP) phase transition and the U^{33} slopes of the carboxylic group's oxygen increase by half at the phase transition. This is related to the number and strength of intermolecular interactions involving these oxygen atoms. Furthermore, it is of interest to note that, in the HT phase, the N1 ammonium atom has the same behaviour as O3 in the **c** direction. That means that N1 and O3 displacements along **c** are related and suggests some relationship between the vibrational behaviour of the N1 and O3 atoms via the (N1...O3) hydrogen bond. Indeed, the strengthening of the latter in the **c** direction may enhance the cooperativity between N1 and O3 in the LTP.

The phenyl ring does not show any significant variation, and displacement parameters behave similarly in both phases.

Table 3.The values of the rigid-body T (\AA^2), L (deg^2) and S (rad \AA) of the phosphite anion at 100 K and 293 K.

	100 K	293 K
T (\AA^2)	T11 = 0,011(6) T12 = 0,001(5) T13 = -0,003(5) T22 = 0,001(7) T23 = -0,001(5) T33 = 0,011(5)	T11 = 0,031(5) T12 = -0,006(4) T13 = -0,008(5) T22 = 0,041(5) T23 = 0,002(5) T33 = 0,035(4)
L ($\text{^{\circ}2}$)	L11 = 13(17) L12 = 25(20) L13 = 1(28) L22 = 4(26) L23 = -3(12) L33 = 16(26)	L11 = 62(10) L12 = 52(16) L13 = -15(28) L22 = 58(22) L23 = -17(12) L33 = 55(18)
S (rad \AA)	S11 = -0,002(3) S12 = -0,001(5) S13 = -0,001(4) S21 = 0,001(3) S22 = -0,001(4) S23 = -0,000(3) S31 = -0,006(6) S32 = -0,001(2) S33 = 0,003(5)	S11 = -0,000(2) S12 = 0,002(5) S13 = 0,003(4) S21 = 0,001(2) S22 = 0,001(4) S23 = -0,001(2) S31 = -0,001(5) S32 = -0,005(2) S33 = -0,000(4)
Rw	0,19	0,07

$$Rw = [\sum w(U_{\text{obs}}^{ij} - U_{\text{cal}}^{ij})^2 / \sum w(U_{\text{obs}}^{ij})^2]^{1/2}; w = \sigma[\langle U_{\text{obs}}^{ij} \rangle]^{-2}$$